Collective effects in intersubband transitions

R.J. Warburton[a, *], K. Weilhammer[a], C. Jabs[a], J.P. Kotthaus[a], M. Thomas[b], H. Kroemer[b]

[a] *Center for NanoScience and Sektion Physik, LMU, Geschwister-Scholl-Platz 1,*
80539 München, Germany
[b] *Department of Electrical and Computer Engineering, University of California, Santa Barbara, CA 93106, USA*

Abstract

We present experiments on the intersubband resonance (ISR) in InAs/AlSb quantum wells with the aim of understanding the linewidth. We find that fluctuations in the well width dominate the scattering right up to temperatures well beyond room temperature. ISR with two occupied subbands is used to gain insight into these phenomena. We find clear evidence for Landau damping and we argue generally that Landau damping represents the crucial scattering mechanism for all ISRs. The argument is strengthened by considering the intrasubband plasmon, where we also find evidence for Landau damping, in this case in a magnetic field. © 2000 Elsevier Science B.V. All rights reserved.

Keywords: Intersubband resonance; Linewidth; Collective effects; InAs

1. Introduction

It has been known for at least 20 years that intersubband resonance (ISR) is not a single-particle process [1,2]. ISR is a collective phenomenon, more accurately described as a plasmon or charge-density excitation. There are now a number of experiments which demonstrate this point. One example is the ISR in a system with a broad single-particle density of states. This can be achieved in a low-band-gap system such as InAs where the separation between the subbands is smaller at the Fermi wave vector $k = k_f$ than at $k = 0$. In such a case, the ISR is a single, narrow

line: the collective effects collapse all the available oscillator strength into a single mode [3–5]. Another example is to probe the ISR in the non-linear regime with a very intense source. In this case, optical pumping of the carriers weakens the collective effects and the ISR red-shifts [6].

The collective effects shift the energy away from the single-particle energy separating the subbands. This shift however represents typically only a small proportion of the ISR energy as there are two competing effects. The direct electron–electron interaction, often referred to as the depolarisation field in this context, and the exchange–correlation interaction cause blue- and red-shifts, respectively, and tend to cancel [7,8]. This enables the ISR energy to be estimated to the 10% level simply with a single-particle calculation. It is now widespread practice to model all ISRs, in

* Corresponding author. Fax: +49-89-2180-3182.
E-mail address: richard.warburton@physik.uni-muenchen.de (R.J. Warburton)

particular in ISR-based emitters and detectors, with the single-particle states. While this approach may be satisfactory for the ISR energy we argue here that it is very misleading for the scattering mechanisms which determine the ISR linewidth.

The purpose of the present work is to examine the linewidth of the ISR. In the best samples, the ISR linewidth is homogeneously broadened, in which case the linewidth is determined by scattering mechanisms [9,10]. In another terminology, the linewidth is inversely related to the dephasing time of the ISR. There exist some experimental studies of the linewidth: it would appear that the linewidth is determined by elastic, momentum non-conserving scattering off extrinsic defects such as interface roughness or ionised impurities [10]. The temperature dependence has not been extensively explored, but there are some reports that at least for GaAs-based devices the room temperature linewidth is comparable to the low-temperature linewidth [11–13]. Furthermore, the ISR linewidth has no obvious correlation with the transport mobility [10]. Theoretically, we are not aware of a microscopic approach to compute the linewidth. In fact, the ISR linewidth is usually described with the single-particle scattering rates.

We present here a detailed study of ISR of InAs/AlSb quantum wells. We find that the ISR linewidth rises strongly with reducing well width but has a very weak temperature dependence. We argue that the weak temperature dependence cannot be easily understood in a single-particle picture. Instead, we propose a collective picture based on Landau damping. This model is supported by experiments on a quantum well with two occupied subbands where we see the direct consequences of Landau damping [14]. We also present results on the intrasubband plasmon which support our assertion that Landau damping is the crucial scattering mechanism for plasmons in this material system.

2. Samples and experiments

The InAs quantum wells were all grown on GaAs substrates with AlSb barriers. In order to investigate the well width dependence of the ISR, we looked at a number of samples, each with 12 quantum wells and carrier densities within 10% of 10^{12} cm^{-2}, with well widths 60, 70, 85, 100, 130 and 150 Å. The wells are all δ doped 50 Å away from the interfaces, and the wells are separated by 100 Å of AlSb. One sample has a higher doping concentration and also wider wells, 180 Å. In this case, two subbands are occupied as revealed by a beating in the Shubnikov–de Haas oscillations. By analysing the oscillations we determined the densities of the first and second subbands (labelled 1 and 2) to be $n_1 = 1.89 \times 10^{12}$ cm^{-2} and $n_2 = 0.74 \times 10^{12}$ cm^{-2}, respectively. We have also investigated an additional sample with a single 150 Å InAs quantum well with carrier density 0.9×10^{12} cm^{-2} and particularly high mobility, ca. 0.5×10^6 cm^2/V s.

The ISR was excited in three different ways. The first technique was simply to tilt the sample with respect to the incident beam (loosely referred to as Brewster geometry). The second technique was to deposit a thick layer of silver onto the sample surface and to illuminate the bevelled edges of the sample (strip-line geometry). This tended to give very strong resonances and in some cases we deposited only a 0.2 mm wide strip of silver in order to avoid saturation effects. The third technique was to use crossed electric and magnetic field (Voigt geometry) [15]. The magnetic field (up to 12 T) lies in the plane of the quantum well as does the electric field of the light. This geometry gives much weaker resonances than in the strip-line geometry, ruling out saturation effects, and allows the ISR matrix element to be determined simply from the resonance intensity.

The ISRs lie in the mid infrared and were recorded with a Fourier transform spectrometer and variety of detectors (low-temperature Ge : Cu photoconductor, HgCdTe photoconductor and a DLTS detector). A reference spectrum was taken at normal incidence (Brewster geometry), from a sample with a different well width (strip-line geometry), or at zero magnetic field (Voigt geometry).

Related to the ISR is the intrasubband plasmon. However, the energy of the intrasubband plasmon is zero at zero wave vector, and so in order to excite a plasmon we supplied an additional impulse with a metallic grating on the sample surface. The intrasubband plasmon has a much smaller energy than the intersubband plasmon corresponding to wavelengths in the far-infrared region which we detected with a 2 K composite Si bolometer.
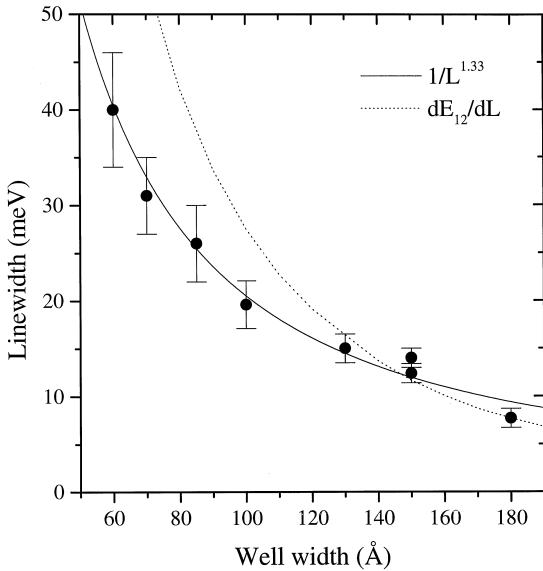
Fig. 1. The linewidth of the intersubband resonance (ISR) against well width. The solid symbols represent the measurements on InAs/AlSb quantum wells at 4.2 K with electron densities around 10^{12} cm^{-2}. The dotted curve is $\Gamma \propto dE_{12}/dL$ where the separation between the first and second subbands E_{12} was calculated with the Kane model, and the curve was made to pass through the point for well-width 180 Å. The solid curve is a fit to the experimental data.

For both the ISR and the intrasubband plasmon, the experimental resonances are close to Lorentzian in shape and we therefore infer that the broadening is predominantly homogeneous.

3. The intersubband resonance

3.1. Temperature and well-width dependence of the linewidth

Fig. 1 shows the linewidth of the ISR plotted against well width for a temperature of 4.2 K. It can be seen that the linewidth rises quite rapidly with decreasing well width. The most obvious explanation is that well width fluctuations are responsible for the linewidth because they increase in importance as the well narrows. Other possible scattering mechanisms, for instance off ionised impurities and phonons, would not have such a strong well-width dependence. Fig. 2 shows the linewidth against temperature for the sample with 180
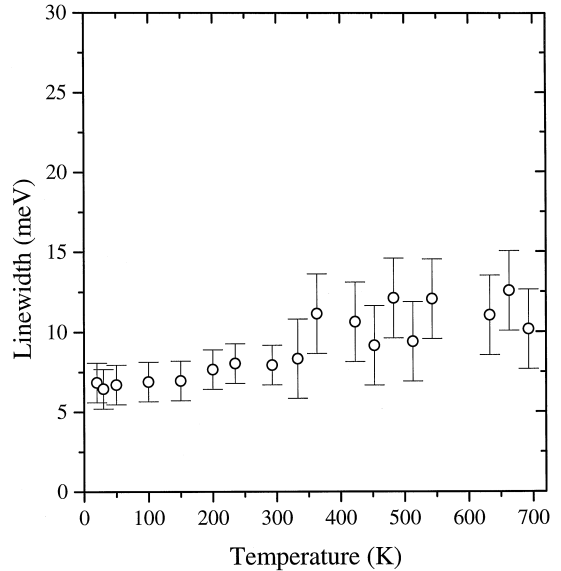

Fig. 2. The ISR linewidth for a 180 Å quantum well with 2.63×10^{12} cm^{-2} carrier density plotted against temperature. Note that the temperature scale extends to well above room temperature.

Å well width. [1] It can be seen that the linewidth is remarkably insensitive to temperature, increasing by barely 50% right up to 700 K, i.e. well above room temperature. It can therefore be concluded that scattering off well-width fluctuations is the dominant dephasing mechanism even at high temperature. As in Ref. [10] we find no correspondence of the intersubband lifetime with the transport mobility. At low temperature for instance we have two samples with 150 Å well width with transport mobilities differing by an order of magnitude. Nevertheless, the ISR linewidths differ by no more than 10%. As the temperature increases, the transport mobility decreases rapidly as scattering off LO phonons becomes more prevalent yet the ISR linewidth is largely unchanged.

It is difficult to account for the dependence of the ISR linewidth on well width and its independence on temperature in a single-particle model. At low temperature, one would naively expect that the linewidth increases as $1/L^3$. This is too strong a dependence on well width, partly due to the neglect of

---

[1] Plotted in Fig. 2 is the linewidth of the 2–3 ISR of the sample with two occupied subbands. The sample with 150 Å well width and a singly occupied subband showed essentially the same behaviour.
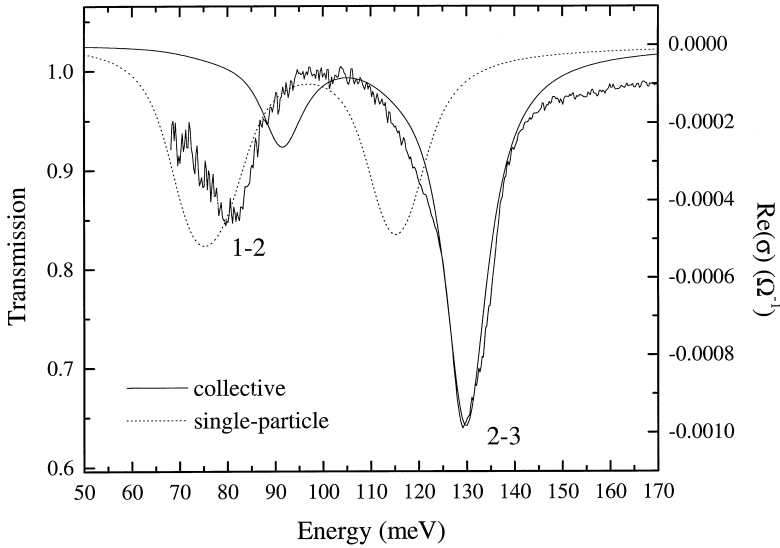
Fig. 3. The measured ISR for a 180 Å InAs quantum well with two occupied subbands. Results of the calculations are also shown: the dotted curve is without collective effects; the solid curve includes collective effects in the self-consistent field approximation (Ando model).

the nonparabolicity in the InAs band structure which weakens the well-width dependence. It is straightforward to incorporate the nonparabolicity with the Kane model [4] and this yields the dotted curve in Fig. 1. The curve rises more rapidly than the experimental data points and this represents a failure of the single-particle picture. The temperature dependence is still more striking. All estimates of the ISR linewidth from LO phonon scattering are in the range of a few meV [9,16]. On increasing the temperature, the LO phonon emission rate should increase as $1 + n_{LO}$ where n_{LO} is the LO phonon occupation. This factor doubles between 0 and 600 K. Furthermore, absorption of LO phonons should also contribute to the linewidth at elevated temperatures. In other words, in a single-particle picture the ISR linewidth should show a much stronger dependence on temperature than is observed experimentally.

3.2. ISR for two occupied subbands

In order to probe this issue further, we present the ISRs of the sample with two occupied subbands. The transmission spectrum at low temperature is shown in Fig. 3. There are two resonances as expected, one corresponding to the 1–2 ISR, and one to the 2–3 ISR.

It is interesting to note that the 1–2 ISR is weaker than the 2–3 ISR and we first discuss this point.

In a single-particle picture, the oscillator strength of the 1–2 ISR is proportional to $(n_1 - n_2)z_{12}^2E_{12}$ and the oscillator strength of the 2–3 ISR is proportional to $n_2 z_{23}^2 E_{23} z_{12}$ (z_{23}) is z-dipole matrix element element between the first and second (second and third) subbands. For the present sample, $(n_1 - n_2) > n_2$ and the matrix elements z_{12} and z_{23} are approximately equal. (Including band nonparabolicity, we calculate $z_{12} = 36.5$ and $z_{23} = 39.5$ Å). Hence, in the single-particle picture the 1–2 : 2–3 intensity ratio should be 1.3 : 1. In the experiment however, the ratio is 0.5 : 1. The explanation is that the depolarisation field not only shifts both the 1–2 and 2–3 ISRs to higher energy but it also couples the two resonances. An analogy with two coupled pendulums can be made: there is an in-phase normal mode (2–3) and an out-of-phase normal mode (1–2). The out-of-phase mode couples weakly to the long wavelength electric field of the light. A sum rule on the oscillator strength is bound to exist so that the 2–3 ISR gains intensity from the 1–2 ISR. It should be noted that the terminology 1–2 and 2–3 is only approximate as the depolarisation field admixes the two ISRs. As the carrier intensity increases, the coupling becomes stronger such that the 2–3 mode takes es-
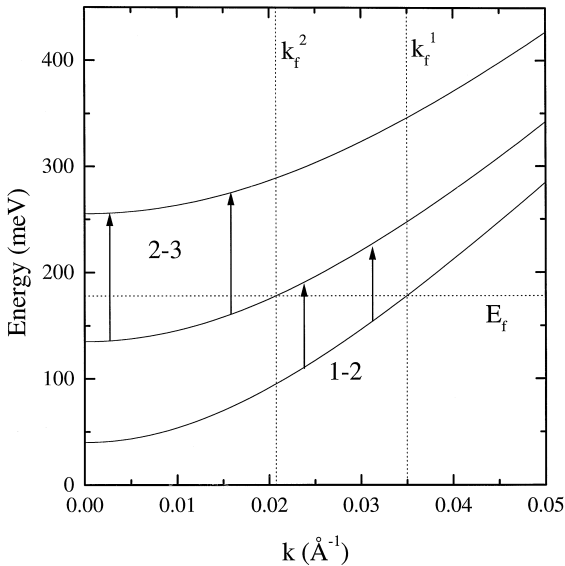
Fig. 4. The in-plane dispersion of the subbands in a 180 Å InAs/AlSb quantum well calculated with four band $\boldsymbol{k} \cdot \boldsymbol{p}$ theory. Static many-electron effects have been neglected. The low-temperature Fermi energy E_f and the corresponding Fermi wave vectors k_f^1 and k_f^2 are shown as dotted lines. The energy zero lies at the bottom of the InAs well.

sentially all of the oscillator strength. This is exactly what is observed: at 6×10^{12} cm^{-2} for instance we can only observe a single ISR.

The claim is that the depolarisation field not only quenches the broadening in the single-particle spectrum but also transfers oscillator strength from the 1–2-like ISR to the 2–3-like ISR. To confirm this point, we have carried out calculations in the Ando formalism (self-consistent field approximation) [2]. The formalism was extended to include both multiply occupied subbands and elevated temperatures. At the carrier densities here, the depolarisation field is the dominant collective interaction so for simplicity we have neglected the exciton term. The single-particle states were calculated with the Kane model and their dispersions are shown in Fig. 4. As a check, we fixed the Fermi energy such that the total carrier concentration is $n_1 + n_2 = 2.63 \times 10^{12}$ cm^{-2}, the experimental value, and compared the calculated $n_1 : n_2$ ratio to the experimental one. The agreement was better than 10%. The Ando theory assumes that all single-particle states have an inhomogeneous width Γ which is state

and temperature independent. The calculation gives most directly the real part of the out-of-plane dynamic conductivity $\Re(\sigma_{zz}(E))$ at zero wave vector $q = 0$. This is linearly related to the absorption; $-\Re(\sigma_{zz}(E))$ can be directly compared to the transmission data.

Fig. 3 shows the results of the calculations taking $\Gamma = 11$ meV to reproduce the experimental linewidth. [2] At low temperature, we have an excellent agreement with the experimental results supporting the claim that the depolarisation field is responsible for the transfer of intensity from 1–2 to 2–3. The only discrepancy between the calculated and measured spectra is the energy of the 1–2-like mode which is perhaps related to the omission of exchange–correlation effects.

We now turn to the temperature dependence. The experimental data are shown in Fig. 5a. It can be seen that the upper 2–3-like ISR has a linewidth which is only weakly temperature dependent right up to 600 K. Conversely, the lower 1–2-like ISR broadens above 200 K and eventually forms a shoulder of the 2–3-like ISR. Our explanation is that the lower mode becomes degenerate with single-particle transitions as the temperature is increased and this degeneracy dephases the ISR. This is an example of Landau damping which is known from metal physics to be a very effective scatterer of plasma oscillations [17]. In this case, the single-particle transitions are between subbands 2 and 3 at high k which have a low energy because of band nonparabolicity.

Calculations with the Ando formalism reproduce the experimental results very closely, as shown in Fig. 5b. As in the experiment, the lower ISR broadens above 200 K. To confirm our interpretation of Landau damping, we plot in Fig. 6 $\Re(\sigma_{zz})$ against energy without collective effects. There are two main peaks corresponding simply to the 1–2 and 2–3 intersubband transitions. The peaks are broad due to both the assumed inhomogeneous broadening and the nonparabolicity in the band structure. The calculated energies of the collective modes are shown by the dotted lines. It can be seen that at the 2–3 collective ISR,

---

[2] The line width of the 2–3 ISR is ca. 11 meV in this strip-line experiment and is slightly larger than the width determined from the same sample in the Voigt geometry (plotted in Figs. 1 and 2). This is because saturation effects in the strip-line geometry could not be eliminated completely.
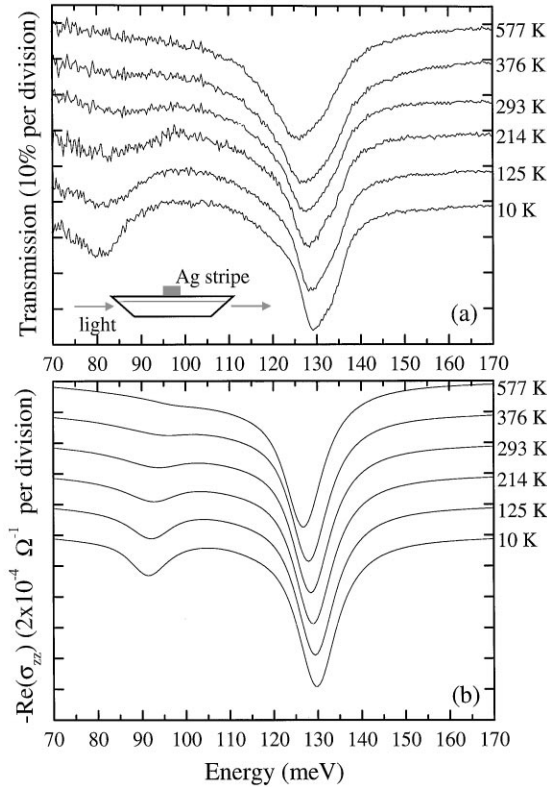
Fig. 5. The temperature dependence of the ISR for the 180 Å InAs quantum well with two occupied subbands: (a) experimental transmission spectra. The spectra are offset from 1 for the various temperatures; (b) calculations of the real part of the dynamic conductivity, σ_{zz}, at zero wave vector in the Ando model. The curves are offset from 0 for clarity.

Fig. 6. The calculated real part of the dynamic conductivity, σ_{zz}, without collective effects at three different temperatures. The curves correspond to the density of single-particle transitions with $q = 0$ which form the single-particle background density of states for the calculations in Fig. 5b. The two dotted lines show the energies of the calculated 1–2 and 2–3 collective modes at low temperature.

there is almost no change on increasing the temperature. However, at the energy of the 1–2 collective ISR, the single-particle density of states increases rapidly with increasing temperature. This supports the Landau damping interpretation.

3.3. Discussion of the ISR linewidth

Experiments on the sample with two occupied subbands show that Landau damping represents a strong scattering mechanism of the ISR. In the experiment, the 1–2 mode broadens because it is Landau damped; the 2–3 mode remains sharp because it is not. It is possible to explain, at least qualitatively, the experimental results against temperature and well width also with
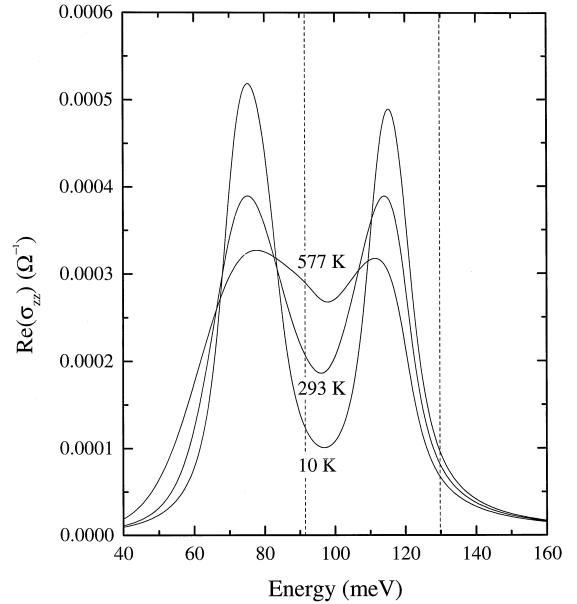
Landau damping. The starting point is the dispersion relation of the ISR and the underlying single-particle transitions, as shown in Fig. 7 for the simple case of an InAs/AlSb quantum well with a singly occupied subband. The ISR has a very weak dispersion. The single-particle transitions correspond to all possible transitions between occupied and unoccupied states and fall into bands as shown. A number of points can be made with this diagram.

First, the ISR is isolated from the single-particle transitions at $q = 0$. This means that in a pure system, Landau damping cannot take place, i.e. the resonance should be sharp. This is exactly what is observed. Secondly, it is clear why scattering of the ISR with phonons is ineffective. A phonon can only scatter the ISR along its dispersion relation and this severely limits the number of phonons which can participate. Thirdly, an increase of temperature causes states at higher k to be occupied where the subbands are separated by smaller energies through band nonparabolicity. This smears the band of single-particle transitions
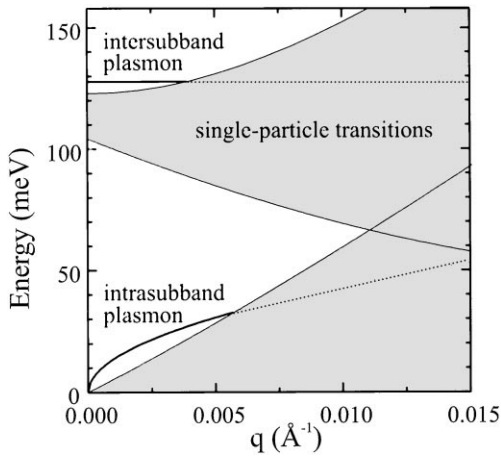
Fig. 7. The energy of the collective modes, the ISR and intrasubband plasmon, against in-plane wave vector, q, along with the single-particle transitions (shaded areas) for a 150 Å InAs/AlSb quantum well with a singly occupied subband with electron density 10^{12} cm^{-2}.

Fig. 8. Transmission spectra of a 150 Å InAs/AlSb quantum well with electron density 10^{12} cm^{-2} with a metallic grating on the sample surface. The grating has period 1 μm with 0.5 μm thick stripes. The spectra were recorded at various temperatures and are offset from 1 for clarity.

to lower energies. The important point however is that the ISR mode at $q = 0$ lies above the single-particle transitions and so never becomes degenerate with them, even at very high temperature. This, along with the comment concerning phonon scattering, explains the robustness of the ISR at high temperature. Fourthly, the strong well-width dependence can also be accommodated within this model. Short-range fluctuations in the plane with characteristic length ΔL imply an uncertainty in the in-plane ISR wave vector of $\Delta q \sim \pi/\Delta L$. If this Δq is large enough, the ISR moves into a part of its dispersion where Landau damping occurs. The strong well-width dependence arises from the fact that the depolarisation shift decreases with well width, implying that the mode at $q = 0$ is energetically close to the single-particle states at $q = 0$ for a narrow well. This also means that the intersection of the ISR dispersion curve with the band of single-particle states occurs at smaller q. In other words, a given Δq is more effective in scattering the ISR for a narrow well than for a wide well. Finally, this collective picture is quite different from the usual considerations used to describe the transport mobility where scattering events which degrade the forward momentum are important. It is then no surprise that the ISR linewidth and transport mobility show no obvious correlation.
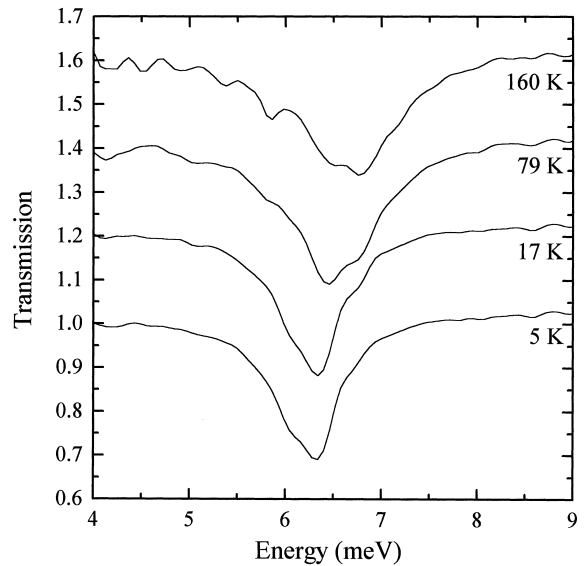
4. The intrasubband plasmon

Fig. 7 shows that there is another plasmon mode in this system in addition to the ISR. This is the intrasubband plasmon which involves excitations only in the occupied subbands and is therefore analogous to plasmons in conventional metals. However, as the subbands are two-dimensional, the dispersion takes on a particular form, varying as $\sqrt{q}$. We excited a plasmon at $q = 2\pi/d$ with a metallic grating of period d on the sample surface. Fig. 8 shows the transmission of a sample with 1 μm grating on the surface at zero magnetic field ($B = 0$) for several temperatures. The mode at ca. 6 meV is the intrasubband plasmon.

Fig. 8 illustrates that the intrasubband plasmon survives right up to 160 K. It is not as robust at elevated temperatures as the ISR, but at low temperature the intrasubband plasmon does have a smaller linewidth than the ISR. Fig. 9 shows the behaviour of the intrasubband plasmon in a magnetic field, in this case for a sample with 6 μm grating period where in fact at least two intrasubband plasmons can be excited. The strong absorption which increases in energy with increasing

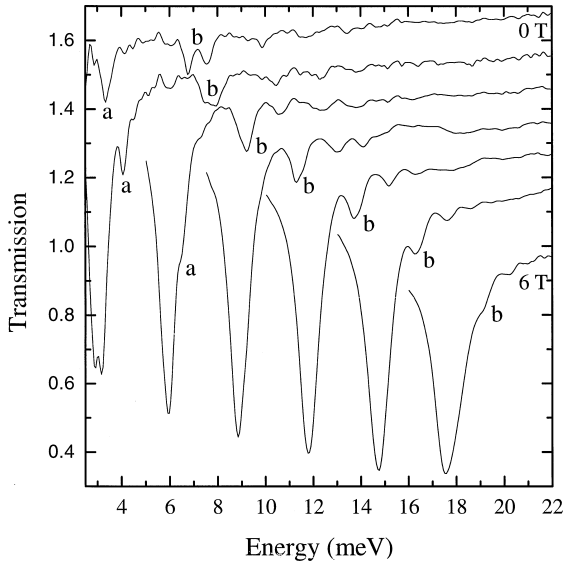Fig. 9. Transmission spectra of a 150 Å InAs/AlSb quantum well at 4.2 K with electron density 10^{12} cm^{-2} with a metallic grating on the sample surface. The grating has period 6 μm with 3 μm thick stripes. The data were recorded at magnetic fields 0, 1, 2, 3, 4, 5, and 6 T. The curves are offset from 1 for clarity.

interpretation is that these processes scatter the ISR along its dispersion curve into a region where the ISR is strongly damped. Following this train of thought, this is less likely to happen to the intrasubband plasmon because its dispersion has a much stronger dependence on wave vector. This would explain why at low temperature the intrasubband plasmon has a smaller linewidth than the ISR. In a magnetic field, the single-particle structure is changed: the available density of states is concentrated into Landau levels. Damping of the intrasubband plasmon can then occur through a degeneracy with transitions between the Landau levels (essentially cyclotron resonance). As the magnetic field increases, the intrasubband plasmon becomes closer energetically to the cyclotron resonance, increasing the damping.

These results are significant as they can be interpreted with the same picture as those on the ISR despite the different energies and dispersions of the two excitations. The two modes are clearly related. It is known for instance that the intrasubband plasmon and the ISR repel each other energetically [18,19]. This simply emphasises the point that the ISR is a form of plasma oscillation and not simply the transition between two quantum states.

magnetic field is simply the electron–cyclotron resonance. Plasmon a merges with the cyclotron resonance around 2 T; plasmon b at around 6 T. If the plasmons maintained their $B = 0$ linewidths they would be strong enough to be distinguishable from the cyclotron resonance. The results in Fig. 9 imply rather that the plasmons broaden when they are close to the cyclotron resonance. All these effects can be intrepreted in terms of Landau damping.

The intrasubband plasmon at low temperature and $B = 0$ T is energetically separated from the single-particle transitions and therefore exhibits a sharp line. As explained above, the ISR mode at $q = 0$ never becomes degenerate with single-particle excitations and this helps to preserve its character at elevated temperature. However, the intrasubband plasmon does become degenerate with some thermally excited single-particle excitations because it inevitably has a finite q. This means that the intrasubband plasmon is more sensitive to thermal smearing of the Fermi distribution than the ISR. The scattering of the ISR is dominated by elastic, momentum nonconserving processes. Our

5. Conclusions

We have investigated the linewidth of the ISR in InAs/AlSb quantum wells. Experimentally, the linewidth increases with decreasing well width but exhibits only modest changes with increasing temperature even at temperatures well above room temperature. The implication is that well-width fluctuations represent the dominant scattering mechanism at all temperatures. The corollary is that well-width fluctuations must be minimised for the smallest linewidths and optimum device performance. We cannot account for these results on the linewidth with a single-particle model. Instead, we argue that the ISR linewidth is strongly influenced by the collective nature of the ISR. We propose a model based on Landau damping which is inspired by experiments on a sample with two occupied subbands. The model can at least qualitatively account for the experimental results.

Acknowledgements

References

[1] S.J. Allen et al., Solid State Commun. 20 (1976) 425.
[2] T. Ando, Z. Physik B 26 (1977) 263.
[3] C. Gauer et al., Phys. Rev. Lett. 74 (1995) 2772.
[4] R.J. Warburton et al., Phys. Rev. B 53 (1996) 7903.
[5] M. Załużny, Phys. Rev. B 43 (1991) 4511.
[6] K. Craig et al., Phys. Rev. Lett. 76 (1996) 2382.
[7] W.L. Bloss, J. Appl. Phys. 66 (1989) 3639.
[8] E. Batke et al., Phys. Rev. B 43 (1991) 6812.
[9] J. Faist et al., Appl. Phys. Lett. 63 (1993) 1354.
[10] K.L. Campman et al., Appl. Phys. Lett. 69 (1996) 2554.
[11] P. von Allmen et al., Semicond. Sci. Technol. 3 (1988) 1211.
[12] M.O. Manasreh et al., Appl. Phys. Lett. 57 (1990) 1790.
[13] D. Huang et al., Phys. Rev. B 52 (1995) 14 126.
[14] R.J. Warburton et al., Phys. Rev. Lett. 80 (1998) 2185.
[15] C. Gauer et al., Europhys. Lett. 30 (1995) 111.
[16] R. Ferreira, G. Bastard, Phys. Rev. B 40 (1989) 1074.
[17] G.D. Mahan, Many-Particle Physics, Plenum Press, New York, 1993 (Chapter 5).
[18] S. Das Sarmar, Phys. Rev. B 29 (1984) 2334.
[19] S. Oelting et al., Phys. Rev. Lett. 56 (1986) 1846.